Excluded-Volume Effects on the Hydrodynamic Radius of Oligo- and Polystyrenes in Dilute Solution

Toshihiro Arai, Fumiaki Abe, Takenao Yoshizaki, Yoshiyuki Einaga, and Hiromi Yamakawa*

Department of Polymer Chemistry, Kyoto University, Kyoto 606-01, Japan

Received December 30, 1994; Revised Manuscript Received March 13, 1995[⊗]

ABSTRACT: The translational diffusion coefficient D was determined from dynamic light scattering measurements for atactic polystyrene in toluene at 15.0 °C and in 4-*tert*-butyltoluene at 50.0 °C in the range of weight-average molecular weight M_w from 9.20×10^2 to 3.84×10^6. The hydrodynamic-radius expansion factor α_H was then determined from the values of the hydrodynamic radius R_H defined from D and those of $R_{H,\Theta}$ previously obtained in cyclohexane at Θ. The results show that the effect of chain stiffness on α_H is significant as in the case of the gyration- and viscosity-radius expansion factors α_S and α_η. It is also shown that α_H becomes a function only of the scaled excluded-volume parameter $\tilde{z}$, which is defined in the Yamakawa–Stockmayer–Shimada theory for the helical wormlike chain with excluded volume, irrespective of the solvent condition, indicating that the quasi-two-parameter scheme is valid for α_H as well as for α_S and α_η. The Barrett equation for α_H with $\tilde{z}$ in place of the conventional excluded-volume parameter z gives values appreciably larger than the observed results for $\alpha_H(\tilde{z})$. This disagreement between theory and experiment may be semiquantitatively explained by the new Yamakawa–Yoshizaki theory which takes account of the possible effect of fluctuating hydrodynamic interaction on α_H. It is interesting to find that the present data for α_H happen to follow almost quantitatively the Barrett equation for α_η with $\tilde{z}$ in place of z in the range of M_w studied.

Introduction

In this series of experimental work on the excluded-volume effects in dilute solutions of oligomers and polymers,[1–5] we have shown that a quasi-two-parameter scheme is valid for the gyration- and viscosity-radius expansion factors α_S and α_η for atactic polystyrene (a-PS), polyisobutylene (PIB), atactic poly(methyl methacrylate) (a-PMMA), and isotactic poly(methyl methacrylate) (i-PMMA). That is, both α_S and α_η for them may be expressed as functions only of the scaled excluded-volume parameter $\tilde{z}$ defined in the Yamakawa–Stockmayer–Shimada (YSS) theory[6–8] that takes account of the effects of excluded volume and chain stiffness on the basis of the helical wormlike (HW) chain,[9,10] irrespective of the differences in chain stiffness, local chain conformation, and solvent condition. It has also been shown that $\alpha_S(\tilde{z})$ and $\alpha_\eta(\tilde{z})$ may be explained quantitatively by the Domb–Barrett equation[11] for α_S and approximately by the Barrett equation[12] for α_η, respectively, with $\tilde{z}$ in place of the conventional excluded-volume parameter z. In the present paper, we proceed to make a similar study of the hydrodynamic- (friction-) radius expansion factor α_H for the hydrodynamic radius R_H defined from the translational diffusion coefficient D at infinite dilution, taking a-PS as a first example.

As mentioned in the preceding paper,[13] the literature data for a-PS,[14] *cis*-polyisoprene,[15] and PIB[16] give values of α_H appreciably smaller than the theoretical values calculated from the Barrett equation.[17] A new theory of α_H which takes account of the possible effect of fluctuating hydrodynamic interaction (HI) has there been developed in order to explain this disagreement between theory and experiment. Thus the purpose of the present work is to confirm the literature results and then examine the behavior of α_H as a function of $\tilde{z}$ (and also of α_S) in comparison with the theoretical prediction. In doing this, as in the above studies of α_S and α_η, we have given particular attention to a correct determination of α_H by choosing a proper pair of good and Θ solvents so that the unperturbed dimension in that good solvent may coincide with that in the Θ state taken as a reference standard. In this connection, we note that in the above literature work, no rigorous check of this point has been made in the determination of α_H and also of α_S.

In this work, we determine D from dynamic light scattering (DLS) measurements for a-PS in toluene at 15.0 °C and in 4-*tert*-butyltoluene at 50.0 °C over a wide range of weight-average molecular weight M_w including the oligomer region. As reported previously,[1,18] the unperturbed values $\langle S^2\rangle_0$ of the mean-square radius of gyration $\langle S^2\rangle$ of the a-PS chain in these solvents coincide with the values $\langle S^2\rangle_\Theta$ in cyclohexane at 34.5 °C (Θ). We have already obtained D_Θ or $R_{H,\Theta}$ for a-PS in cyclohexane at Θ in the same range of M_w.[19] Thus we first examine if the unperturbed values $R_{H,0}$ for a-PS in the above good solvents agree with the values $R_{H,\Theta}$ in the oligomer region where the excluded-volume effects may be neglected and then establish experimentally the relation of α_H to α_S (and to α_η) and also α_H as a function of $\tilde{z}$. For a-PS, the values of the HW model parameters required for a determination of $\tilde{z}$ (and also of z) have already been determined from dilute solution properties in the unperturbed state.[1,20,21] As for the excluded-volume strength B for a-PS in toluene at 15.0 °C, we may use the value previously determined from α_S,[1] while we determine it for a-PS in 4-*tert*-butyltoluene at 50.0 °C in this work from the data for α_S previously[18] reported.

Experimental Section

Materials. All the a-PS samples used in this work are the same as those used in the previous studies of the mean-square optical anisotropy $\langle\Gamma^2\rangle$,[20] the intrinsic viscosities $[\eta]_\Theta$[22] and $[\eta]$,[2,3] the mean-square radii of gyration $\langle S^2\rangle_\Theta$[21] and $\langle S^2\rangle$,[1] the transport factors ϱ and Φ,[23] the translational diffusion coefficient D_Θ,[19] and the second virial coefficient A_2 (or the interpenetration function Ψ),[18,24] i.e., the fractions separated by preparative gel permeation chromatography (GPC) or

[⊗] Abstract published in *Advance ACS Abstracts,* April 15, 1995.

0024-9297/95/2228-3609$09.00/0

Table 1. Values of M_w, x_w, and M_w/M_n for Atactic Oligo- and Polystyrenes

sample	M_w	x_w	M_w/M_n
OS8a[a]	9.20×10^2	8.13	1.01
A5000-3[b]	5.38×10^3	51.2	1.03
Fla-2	9.98×10^3	95.4	1.03
F2-2	2.02×10^4	194	1.02
F4	4.00×10^4	384	1.02
F10	9.73×10^4	935	1.02
F20[c]	1.91×10^5	1840	1.02
F40	3.59×10^5	3450	1.01
F80a-2[d]	7.32×10^5	7040	1.03
F128a-2	1.27×10^6	12200	1.03
F380	3.84×10^6	36900	1.05

[a] M_w's of OS8a through F380 had been determined from SLS in cyclohexane at 34.5 °C[1,21,23,24] except for A5000-3, F20, F80a-2, and F128a-2. [b] M_w of A5000-3 had been determined from SLS in methyl ethyl ketone at 25.0 °C.[20] [c] M_w of F20 had been determined from SLS in toluene at 15.0 °C.[1] [d] M_w's of F80a-2 and F128a-2 had been determined from SLS in benzene at 25.0 °C.[3]

fractional precipitation from the standard samples supplied by Tosoh Co., Ltd. All the samples have a fixed stereochemical composition (the fraction of racemic diads $f_r = 0.59$) independent of M_w, possessing an *n*-butyl group at one end of the chain (the initiating end) and a hydrogen atom at the other (the terminating end).

The values of M_w obtained from static light scattering (SLS) measurements and of the weight-average degree of polymerization x_w calculated from them are listed in Table 1 along with those of the ratio of M_w to the number-average molecular weight M_n determined from analytical GPC. Samples F1a-2, F2-2, and F80a-2 may be regarded as the same as F1-2, F2, and F80, respectively, which were used in the previous studies of α_S,[1] α_η,[2,3] and D_Θ.[19] As seen from the values of M_w/M_n, all the samples are sufficiently narrow in molecular weight distribution.

The solvents toluene, 4-*tert*-butyltoluene, and cyclohexane were purified according to standard procedures prior to use.

Dynamic Light Scattering. DLS measurements were carried out to determine D for ten samples in toluene at 15.0 °C, for six samples in 4-*tert*-butyltoluene at 50.0 °C, and for samples F128a-2 and F380 in cyclohexane at 34.5 °C (Θ) by the use of a Brookhaven Instruments Model BI-200SM light scattering goniometer with vertically polarized incident light of 488 nm wavelength from a Spectra-Physics Model 2020 argon ion laser equipped with a Model 583 temperature-stabilized etalon for single-frequency-mode operation. The photomultiplier tube used was EMI 9863B/350, the output from which was processed by a Brookhaven Instruments Model BI2030AT autocorrelator with 264 channels. (An electric shutter was attached to the original detector alignment in order to monitor the dark count automatically.[23]) The normalized autocorrelation function $g^{(2)}(t)$ of the scattered light intensity $I(t)$ at time t was measured at four or five concentrations and at scattering angles θ ranging from 15 to 35°.

From the data for $g^{(2)}(t)$ thus determined at finite concentrations c, we determine D at an infinitely long time[19] at infinite dilution in the same manner as that used in the previous studies.[19,23,25-27] At small c, the plot of $(1/2)\ln[g^{(2)}(t) - 1]$ against t in general follows a straight line represented by

$$(1/2)\ln[g^{(2)}(t) - 1] = \text{const} - At \quad (1)$$

with A the slope for such large t that all the internal motions of solute polymer chains have relaxed away.[25] With the slope A evaluated from the plot, we may determine the apparent diffusion coefficient $D^{(LS)}(c)$ at finite c from

$$D^{(LS)}(c) = \lim_{k \to 0} A/k^2 \quad (2)$$

where k is the magnitude of the scattering vector and is given by

$$k = (4\pi/\tilde{\lambda})\sin(\theta/2) \quad (3)$$

with $\tilde{\lambda}$ the wavelength of the incident light in the solvent. At sufficiently small c, $D^{(LS)}(c)$ may be expanded as

$$D^{(LS)}(c) = D^{(LS)}(0)(1 + k_D^{(LS)}c + ...) \quad (4)$$

so that the desired $D = D(\infty)$ (at an infinitely long time) may be determined from extrapolation of $D^{(LS)}(c)$ to $c = 0$ as

$$D = D^{(LS)}(0) \quad (5)$$

The most concentrated solutions of each sample were prepared gravimetrically and made homogeneous by continuous stirring at room temperature for 1−2 days. They were optically purified by filtration through a Teflon membrane of pore size 0.10−0.45 μm. The solutions of lower concentrations were obtained by successive dilution. The polymer mass concentrations c of the test solutions were calculated from the weight fractions with the densities of the solutions.

The values of the refractive index at 488 nm and the viscosity coefficient η_0 used are 1.513_5 and 0.625_6 cP, respectively, for pure toluene at 15.0 °C and 1.475_8 and 0.772_8 cP, respectively, for pure 4-*tert*-butyltoluene at 50.0 °C. Of these, the value of η_0 of pure toluene is the literature value,[28] and the others were obtained in this work. We note that η_0 of pure 4-*tert*-butyltoluene was measured with a capillary viscometer using pure benzene as a reference, for which the literature value is available.[28]

Static Light Scattering. SLS measurements were carried out to determine $\langle S^2 \rangle$ (and also M_w) for sample F128a-2 in toluene at 15.0 °C, in 4-*tert*-butyltoluene at 50.0 °C, and in cyclohexane at 34.5 °C (Θ). (The results for $\langle S^2 \rangle$ are given in the Discussion section.) The apparatus system, experimental procedure, and method of data analysis are the same as those described in the previous paper.[1]

Viscosity. Viscosity measurements were also carried out for six samples in 4-*tert*-butyltoluene at 50.0 °C and for sample F128a-2 in toluene at 15.0 °C and in cyclohexane at 34.5 °C (Θ) in order to find the relation between α_H and α_η. (The values of α_η in toluene at 15.0 °C had already been obtained.[2]) We used conventional capillary and four-bulb spiral capillary viscometers of the Ubbelohde type. In all the measurements, the flow time was measured to a precision of 0.1 s, keeping the difference between those of the solvent and solution larger than ca. 20 s. The test solutions were maintained at constant temperature within ±0.005 °C during the measurements. The data obtained were treated as usual by the Huggins and Fuoss−Mead plots to determine $[\eta]$ and the Huggins coefficient k'.

The test solutions were prepared in the same manner as in the case of DLS measurements. Density corrections were made in the calculations of c and also of the relative viscosity from the flow times of the solution and solvent.

Results

Translational Diffusion Coefficient. Figure 1 shows plots of $(1/2)\ln[g^{(2)}(t) - 1]$ against t, as examples, for the highest-molecular-weight sample F380 at $c = 1.878 \times 10^{-4}$ g/cm^3 and $\theta = 15°$ (a) and for the lowest-molecular-weight sample OS8a at $c = 0.2042$ g/cm^3 and $\theta = 15°$ (b), both in toluene at 15.0 °C. The data points for each sample follow a straight line over the whole range of t studied except for a few points at small t for the latter, exhibiting no curvature due to internal motions of the chain for the former. Thus the value of A in eq 1 can be determined from its slope with sufficient accuracy. In Figure 2, the values of A/k^2 thus determined are plotted against k^2 for the same samples F380 (a) and OS8a (b) in toluene at 15.0 °C at five and four concentrations, respectively. In the range of k^2 displayed, A/k^2 is almost independent of k^2, so that we adopt as the value of $D^{(LS)}(c)$ $[=(A/k^2)_{k=0}]$ at each finite c the mean value represented by the horizontal straight line. Similarly, we could determine $D^{(LS)}(c)$ for the other

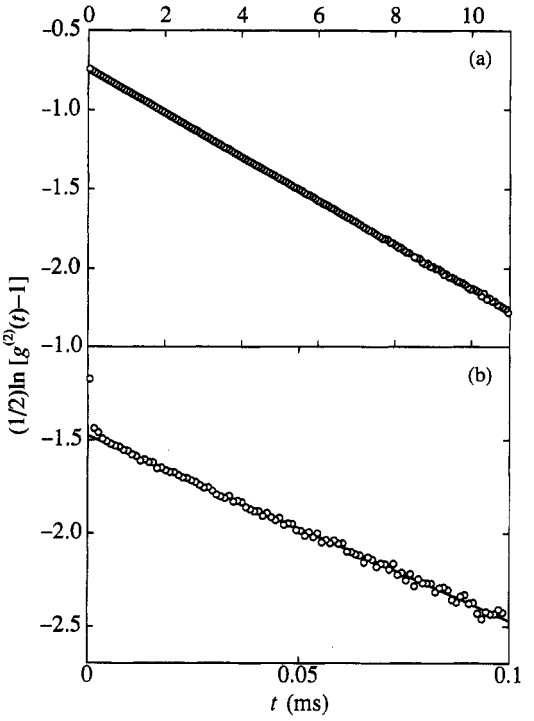

Figure 1. Plots of $(1/2)\ln[g^{(2)}(t) - 1]$ against t for sample F380 at $c = 1.878 \times 10^{-4}$ g/cm^3 and $\theta = 15°$ (a) and for sample OS8a at $c = 0.2042$ g/cm^3 and $\theta = 15°$ (b), both in toluene at 15.0 °C.

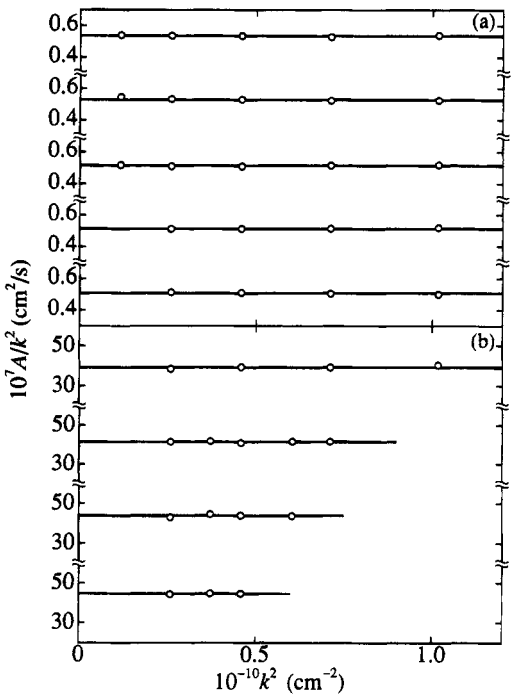

Figure 2. Plots of A/k^2 against k^2 for samples F380 (a) and OS8a (b) in toluene at 15.0 °C. The polymer mass concentrations c are 1.878×10^{-4}, 1.579×10^{-4}, 1.132×10^{-4}, 7.768×10^{-5}, and 4.211×10^{-5} g/cm^3 for F380 and 2.042×10^{-1}, 1.633×10^{-1}, 1.355×10^{-1}, and 1.158×10^{-1} g/cm^3 for OS8a, both from top to bottom.

samples in toluene and also for the six samples examined in 4-*tert*-butyltoluene with sufficient accuracy.

Figures 3 and 4 show plots of $D^{(LS)}(c)$ against c for all the samples examined in toluene at 15.0 °C and in 4-*tert*-butyltoluene at 50.0 °C, respectively. It is seen that the data points for each sample follow a straight line, and thus $D^{(LS)}(0)$ (=D) and $k_D^{(LS)}$ may be accurately

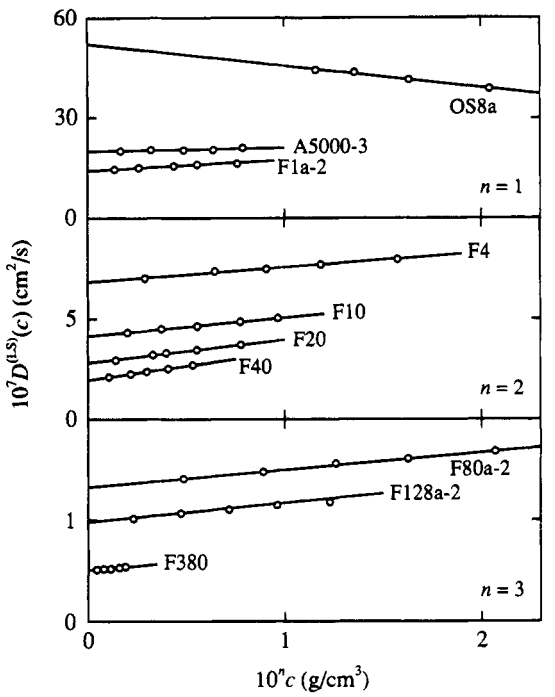

Figure 3. Plots of $D^{(LS)}(c)$ against c for the a-PS samples indicated in toluene at 15.0 °C.

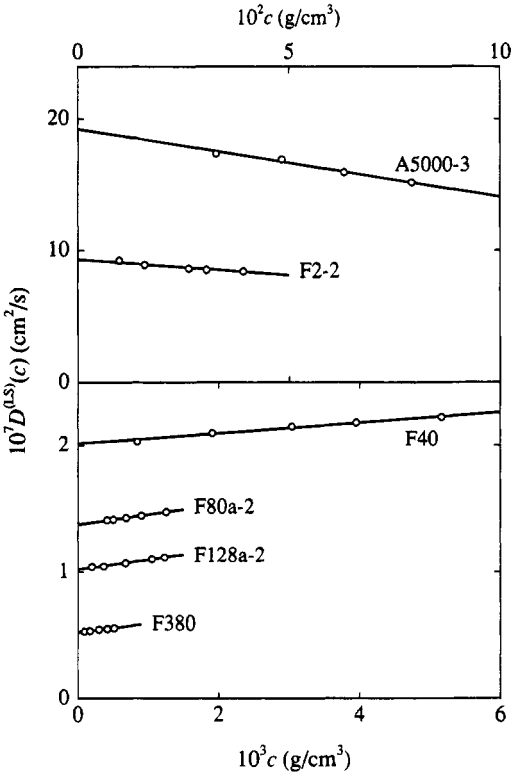

Figure 4. Plots of $D^{(LS)}(c)$ against c for the a-PS samples indicated in 4-*tert*-butyltoluene at 50.0 °C.

determined from its ordinate intercept and slope, respectively. The values of D and $k_D^{(LS)}$ obtained for a-PS in toluene at 15.0 °C and in 4-*tert*-butyltoluene at 50.0 °C are given in Tables 2 and 3, respectively. They also include the values of R_H calculated from the defining equation

$$R_H = k_B T/6\pi\eta_0 D \qquad (6)$$

where k_B is the Boltzmann constant, T is the absolute

Table 2. Results of DLS Measurements for Atactic Oligo- and Polystyrenes in Toluene at 15.0 °C

sample	10^8D, cm²/s	$k_D^{(LS)}$, cm³/g	R_H, Å
OS8a	520	−1.22	6.5
A5000-3	200	0.525	16.9
F1a-2	141	2.38	24.0
F4	68.5	10.7	49.3
F10	41.5	21.8	81.3
F20	28.2	40.6	120
F40	19.6	71.2	172
F80a-2	13.3	130	254
F128a-2	9.78	206	345
F380	5.02	319	672

Table 3. Results of DLS Measurements for Atactic Oligo- and Polystyrenes in 4-*tert*-Butyltoluene at 50.0 °C

sample	10^8D, cm²/s	$k_D^{(LS)}$, cm³/g	R_H, Å
A5000-3	192	−2.69	16.0
F2-2	93.1	−2.44	32.9
F40	20.1	20.4	152
F80a-2	13.8	57.0	222
F128a-2	10.2	77.1	300
F380	5.31	129	577

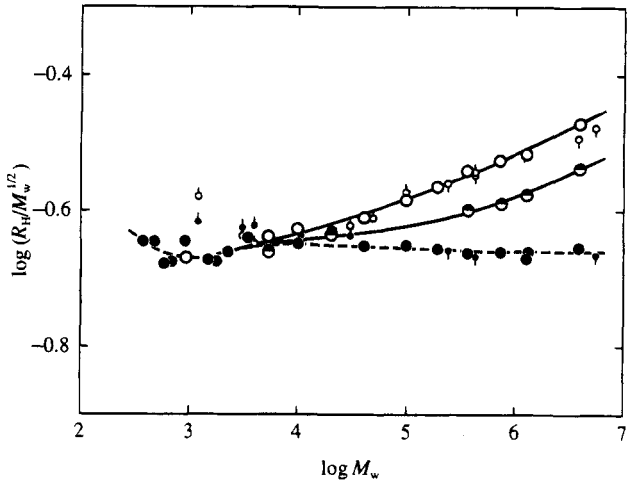

Figure 5. Double-logarithmic plots of $R_H/M_w^{1/2}$ (in Å) against M_w for a-PS: (○) in toluene at 15.0 °C (present data); (◒) in 4-*tert*-butyltoluene at 50.0 °C (present data); (●) in cyclohexane at 34.5 °C (Θ) (present and previous[19,23] data); (○, pip up) in toluene at 20.0 °C (Huber et al.);[29] (●, pip up) in cyclohexane at Θ (Huber et al.);[29] (○, pip down) in toluene at 30.0 °C (Varma et al.);[14] (●, pip down) in cyclohexane at Θ (Varma et al.).[14] The solid and dashed curves connect the data points smoothly.

temperature, and η_0 is the viscosity coefficient of the solvent. Note that the sign of $k_D^{(LS)}$ for a-PS in toluene and in 4-*tert*-butyltoluene is positive except for OS8a in the former solvent and for A5000-3 and F2-2 in the latter, in contrast to the previous results for a-PS,[19,23] poly(dimethylsiloxane),[25] and a- and i-PMMAs[26,27] in the Θ state.

Figure 5 shows double-logarithmic plots of $R_H/M_w^{1/2}$ (in Å) against M_w for a-PS in toluene at 15.0 °C (unfilled circles) and in 4-*tert*-butyltoluene at 50.0 °C (top-half-filled circles). It includes the present and previous[19,23] values of $R_{H,\Theta}$ obtained in cyclohexane at Θ (filled circles), the former being 241 and 435 Å for samples F128a-2 and F380, respectively. It also includes the literature data obtained by Huber et al.[29] for a-PS in toluene at 20.0 °C (unfilled circles with pip up) and in cyclohexane at Θ (filled circles with pip up) and by Varma et al.[14] for a-PS in toluene at 30.0 °C (unfilled circles with pip down) and in cyclohexane at Θ (filled circles with pip down), for comparison. The solid and dashed curves connect the data points smoothly (the latter for the cyclohexane solutions). The present and literature data for a-PS in each solvent agree with each other fairly well except for a few data points for the oligomer samples by Huber et al. The agreement for the toluene solutions indicates that for a-PS in toluene R_H does not significantly depend on temperature.

Table 4. Results of Viscometry for Atactic Oligo- and Polystyrenes in 4-*tert*-Butyltoluene at 50.0 °C

sample	$[\eta]$, dL/g	k'
A5000-3	0.0704	0.57
F2-2	0.137	0.57
F40	0.829	0.38
F80a-2	1.32	0.38
F128a-2	1.87	0.36
F380	4.32	0.36

Table 5. Values of α_H, α_S, and α_η for Atactic Oligo- and Polystyrenes in Toluene at 15.0 °C

sample	α_H	α_S[a]	α_η[b]
A5000-3	1.05	1.07	1.02
F1a-2	1.06	1.07	1.05
F4	1.11	1.18	1.13
F10	1.17		1.20
F20	1.24	1.32	1.26
F40	1.32	1.43	1.32
F80a-2	1.36	1.51	1.39
F128a-2	1.43	1.62	1.44
F380	1.55	1.78	1.59

[a] The values of α_S have been reproduced from ref 1 except for F128a-2 (present work). [b] The values of α_η have been reproduced from ref 2 except for F128a-2 (present work). The previous values of α_S and α_η for F1-2 and F80 are used as those for F1a-2 and F80a-2, respectively.

It is seen that the difference between the values of R_H and $R_{H,\Theta}$, i.e., the excluded-volume effect on R_H becomes appreciable for $M_w > 5.38 \times 10^3$ in toluene at 15.0 °C. This critical value of M_w for the onset of the effect on R_H is in good agreement with the corresponding value estimated from α_η^3 but larger than that from α_S^2 in the same solvent.[1,2] The values of R_H in the two good solvents agree with those of $R_{H,\Theta}$ in the oligomer region for $M_w \lesssim 5.38 \times 10^3$ within experimental error. This agreement implies that $R_{H,0}$ of the unperturbed a-PS chain in these good solvents may be considered to be identical with its $R_{H,\Theta}$ in cyclohexane at Θ. Thus we may calculate correctly α_H for a-PS in toluene and in 4-*tert*-butyltoluene by the use of the values of $R_{H,\Theta}$ in cyclohexane as the reference standards.

Intrinsic Viscosity. The results for the intrinsic viscosity $[\eta]$ and the Huggins coefficient k' for the six a-PS samples in 4-*tert*-butyltoluene at 50.0 °C are summarized in Table 4. The values of $[\eta]$ and k' determined for sample F128a-2 are 2.92 dL/g and 0.34, respectively, in toluene at 15.0 °C and 0.968 dL/g and 0.59, respectively, in cyclohexane at 34.5 °C (Θ). These values of $[\eta]$ are used for the calculation of α_η in the next section. (We note that the values of $[\eta]_\Theta$ for the other samples had already been determined.[2,21-23])

Discussion

Relations of α_H to α_S and α_η. In Tables 5 and 6 are summarized the values of α_H calculated from the equation

$$R_H = R_{H,\Theta}\alpha_H \tag{7}$$

for the a-PS samples in toluene at 15.0 °C and in 4-*tert*-butyltoluene at 50.0 °C, respectively, with the values

Table 6. Values of α_H, α_S, and α_η for Atactic Oligo- and Polystyrene in 4-*tert*-Butyltoluene at 50.0 °C

sample	α_H	α_S[a]	α_η
A5000-3	0.99	1.03	1.02
F2-2	1.03[b]	1.05	1.04
F40	1.17	1.22	1.17
F80a-2	1.19	1.30	1.22
F128a-2	1.25	1.36	1.25
F380	1.33	1.49	1.35

[a] The values of α_S have been reproduced from ref 18 except for F128a-2 (present work). The previous values of α_S for F2 and F80 are used as those for F2-2 and F80a-2, respectively. [b] The value of α_H for F2-2 has been calculated with the value of $R_{H,\Theta}$ interpolated from the previous data.[19]

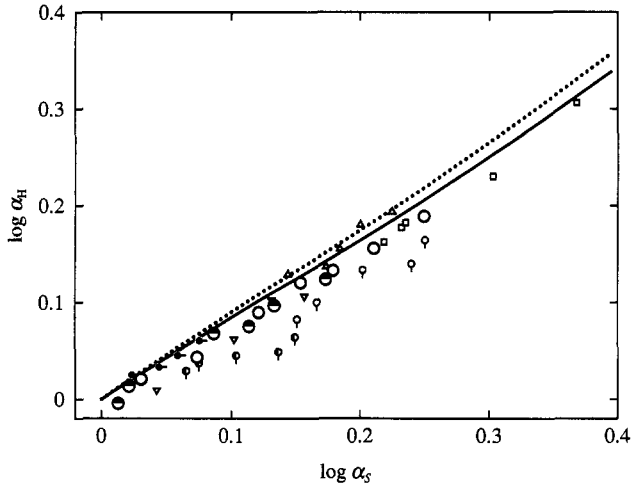

Figure 6. Double-logarithmic plots of α_H against α_S: (○) a-PS in toluene at 15.0 °C (present data); (◓) a-PS in 4-*tert*-butyltoluene at 50.0 °C (present data); (○, pip down) a-PS in toluene at 30.0 °C (Varma et al.);[14] (◐, pip down) a-PS in MEK at 30.0 °C (Varma et al.);[14] (●, pip right) a-PS in cyclohexane at 44.5 °C (Varma et al.);[14] (□) *cis*-polyisoprene in cyclohexane at 35.0 °C (Tsunashima et al.);[15] (△) PIB in cyclohexane at 25.0 °C (Fetters et al.);[16] (▽) PIB in *n*-heptane at 25.0 °C (Fetters et al.).[16] The solid and dotted curves represent the values calculated from eqs 10 and 8, respectively (see text).

of R_H given in Tables 2 and 3 and the values of $R_{H,\Theta}$ given in Table IV of ref 19 except for those determined in this work for samples F128a-2 and F380. The value of α_H for sample F2-2 in 4-*tert*-butyltoluene has been calculated with that of $R_{H,\Theta}$ interpolated from the previous data,[19] since the latter value directly measured was somewhat erroneous. Note that the relation $R_{H,0} = R_{H,\Theta}$ holds for the present polymer–solvent systems. These tables also include the values of α_S and α_η, where those of α_S and α_η in toluene and those of α_S in 4-*tert*-butyltoluene have been reproduced from refs 1, 2, and 18, respectively, except for sample F128a-2, while the values of α_η in 4-*tert*-butyltoluene have been calculated with the values of $[\eta]$ given in Table 4 and those of $[\eta]_\Theta$ given in Table III of ref 2 except for sample F128a-2. For this sample, the values of $[\eta]$ and $[\eta]_\Theta$ are given in the Results section and those of $\langle S^2\rangle^{1/2}$ determined in this work are 510, 428, and 314 Å in toluene at 15.0 °C, in 4-*tert*-butyltoluene at 50.0 °C, and in cyclohexane at 34.5 °C (Θ), respectively.

Figure 6 shows double-logarithmic plots of α_H against α_S for a-PS in toluene at 15.0 °C (unfilled circles) and in 4-*tert*-butyltoluene at 50.0 °C (top-half-filled circles). It also includes the data obtained by Varma et al.[14] for a-PS in toluene at 30.0 °C (unfilled circles with pip down), in methyl ethyl ketone (MEK) at 30.0 °C (left-half-filled circles with pip down), and in cyclohexane at 44.5 °C (filled circles with pip right), by Tsunashima et al.[15] for *cis*-polyisoprene in cyclohexane at 25.0 °C (squares), and by Fetters et al.[16] for PIB in cyclohexane at 25.0 °C (triangles up) and in *n*-heptane at 25.0 °C (triangles down). The data obtained by Huber et al.[29] for a-PS in toluene have been omitted in this figure, since they scatter remarkably. We again note that these literature values of α_H and α_S have been determined as usual without confirming the fulfillment of the criteria $R_{H,0} = R_{H,\Theta}$ and $\langle S^2\rangle_0 = \langle S^2\rangle_\Theta$. The dotted curve represents the values calculated from the Barrett equation[17] for α_H

$$\alpha_H = (1 + 6.09z + 3.59z^2)^{0.1} \tag{8}$$

and the Domb–Barrett equation[11] for α_S^2

$$\alpha_S^2 = [1 + 10z + (70\pi/9 + 10/3)z^2 + 8\pi^{3/2}z^3]^{2/15} \times [0.933 + 0.067\exp(-0.85z - 1.39z^2)] \tag{9}$$

The solid curve represents the values calculated from the new theory presented in the preceding paper[13] and described below.

It is clearly seen that the data points culled from the literature deviate downward from the dotted curve except for those for PIB in cyclohexane, although they scatter somewhat. The present data for a-PS also exhibit similar deviation, in accordance with the literature results. In order to solve this problem, Yamakawa and Yoshizaki[13] have developed the new theory of α_H by taking account of the possible effect of fluctuating HI on α_H. Their equation for α_H reads

$$\alpha_H = \alpha_H^{(Z)} f_H \tag{10}$$

where $\alpha_H^{(Z)}$ may be given by eq 8 and f_H is given by

$$f_H = \frac{1 - \delta_{1,0}(d/a)}{1 - \delta_{1,0}(d/a\alpha_S)} \tag{11}$$

with

$$\delta_{1,0}(x) = 0.12x^{0.43} \qquad (0 < x < 1) \tag{12}$$

and with d being the bead diameter and a being the effective bond length. The values represented by the solid curve in Figure 6 have been calculated from eq 10 with eqs 8 (for $\alpha_H^{(Z)}$), 11, and 12 with the use of eq 9 for α_S, taking $d/a = 1$ as mentioned in the preceding paper.[13] It is seen that the solid curve shifts downward from the dotted one and approaches the data points more significantly with increasing α_S. However, the new theoretical values of α_H are still somewhat larger than the observed ones. It is also seen that the data points obtained in the present work for a-PS in the two solvents form a single composite curve. Thus we may conclude that at least for a-PS, α_H becomes a function only of α_S irrespective of the solvent used and the molecular weight examined. This leads to the expectation that the quasi-two-parameter scheme may be valid for α_H as well as for α_S and α_η.[1-5]

In order to examine the relation between α_H and α_η, the same data for α_H as in Figure 6 are double-logarithmically plotted against α_η in Figure 7. In the figure, the dashed straight line represents the relation $\alpha_H = \alpha_\eta$ and the dotted and solid curves represent the values of α_H calculated from eqs 8 and 10, respectively,

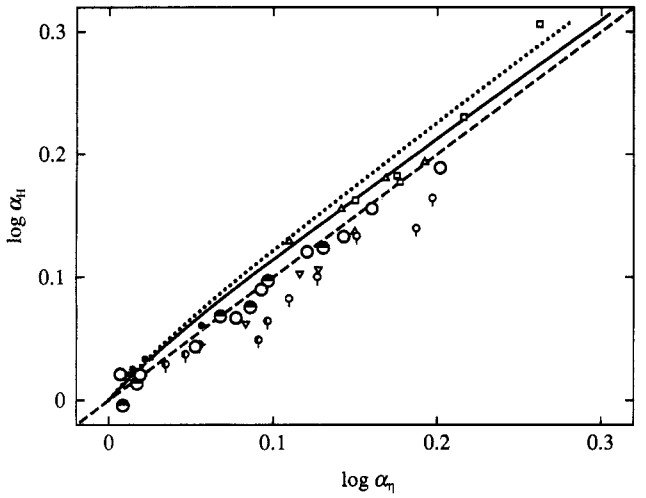

Figure 7. Double-logarithmic plots of α_H against α_η. The symbols have the same meaning as those in Figure 6. The solid and dotted curves represent the values calculated from eqs 10 and 8, respectively (see text). The dashed straight line represents the relation $\alpha_H = \alpha_\eta$.

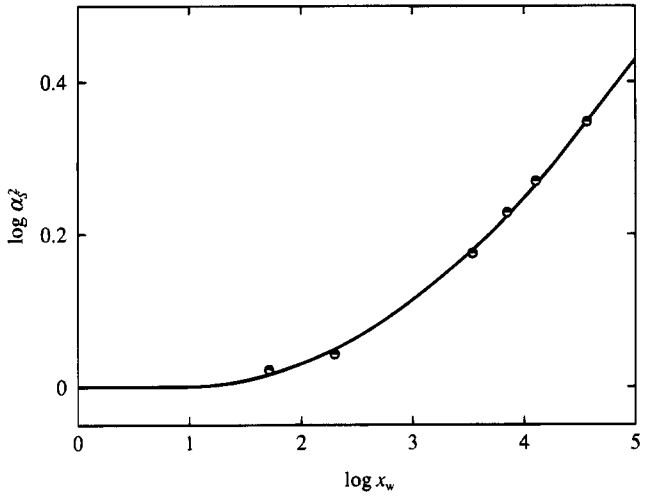

Figure 8. Double-logarithmic plots of α_S^2 against x_w for a-PS in 4-*tert*-butyltoluene at 50.0 °C. The solid curve represents the best-fit YSS theory values (see text).

for the values of α_η calculated from the Barrett equation[12]

$$\alpha_\eta^3 = (1 + 3.8z + 1.9z^2)^{0.3} \tag{13}$$

We must here make a comment on the theoretical values represented by the solid curve, for which the effect of fluctuating HI has been taken into account only for α_H but not for α_η. This is because the effect makes no contribution to $[\eta]$ within the framework of our theory of fluctuating HI on the basis of the HW theory[23] as mentioned in the preceding paper.[13] As in Figure 6, the dotted curve deviates significantly upward from the data points. The values of α_H represented by the solid curve are seen to be closer to the observed ones but still larger than the latter. It is very interesting to see that the present data for a-PS closely follow the dashed line along with the literature ones except for several data points by Varma et al.[14] for a-PS in toluene and in MEK and for the highest data point by Tsunashima et al.[15] for *cis*-polyisoprene, indicating that the relation $\alpha_H = \alpha_\eta$ holds for the polymer–solvent systems examined.

α_H as Functions of z and $\tilde{z}$. As mentioned above, the finding in Figure 6 (and also in Figure 7) implies that α_H for a-PS may be expressed as a function only of $\tilde{z}$ since so are α_S and α_η. Thus it is worthwhile to examine the behavior of α_H as functions of z and $\tilde{z}$ in more detail. For the a-PS samples in toluene at 15.0 °C, we may then use the values of z and $\tilde{z}$ previously[1] determined. However, we must determine the value of the reduced excluded-volume strength λB (see below) for a-PS in 4-*tert*-butyltoluene at 50.0 °C, although we have already established the values of the HW model parameters.[1] For this purpose, the values of α_S^2 are double-logarithmically plotted against x_w in Figure 8 with the data given in Table 6. The solid curve represents the best-fit YSS theory values calculated from eq 9 with $\tilde{z}$ in place of z. Recall that for the HW chain of total contour length L, $\tilde{z}$ is explicitly defined by

$$\tilde{z} = (3/4)K(\lambda L)z \tag{14}$$

and that z is now given by

$$z = (3/2\pi)^{3/2}(\lambda B)(\lambda L)^{1/2} \tag{15}$$

where

$$B = \beta/a^2 c_\infty^{3/2} \tag{16}$$

with

$$c_\infty = \lim_{\lambda L \to \infty} (6\lambda \langle S^2 \rangle_0 / L) = \frac{4 + (\lambda^{-1}\tau_0)^2}{4 + (\lambda^{-1}\kappa_0)^2 + (\lambda^{-1}\tau_0)^2} \tag{17}$$

Here, λ^{-1} is the static stiffness parameter of the HW chain, κ_0 and τ_0 are the differential-geometrical curvature and torsion, respectively, of its characteristic helix taken at the minimum zero of its elastic energy, and β is the binary-cluster integral between beads with a their spacing (effective bond length). In eq 14, the coefficient $K(L)$ is given by

$$K(L) = \frac{4}{3} - 2.711L^{-1/2} + \frac{7}{6}L^{-1} \qquad \text{for } L > 6$$
$$= L^{-1/2}\exp(-6.611L^{-1} + 0.9198 + 0.03516L) \qquad \text{for } L \le 6 \tag{18}$$

Then L is related to the degree of polymerization x by the equation

$$L = xM_0/M_L \tag{19}$$

where M_0 is the molecular weight of the repeat unit of a given real chain and M_L is the shift factor as defined as the molecular weight per unit contour length. The value of λB thus determined from the curve fitting is 0.10. (For a-PS in toluene at 15.0 °C, it has been determined to be 0.26.[1]) The good fit of the data points to the theoretical curve assures that the quasi-two-parameter scheme is valid for a-PS in 4-*tert*-butyltoluene at 50.0 °C.

In Figure 9, the values of α_η^3 are double-logarithmically plotted against $\tilde{z}$ calculated with the values of λB thus determined for a-PS in 4-*tert*-butyltoluene at 50.0 °C (top-half-filled circles). It also includes the previous results[2,3] for a-PS in toluene at 15.0 °C (unfilled circles), in benzene at 25.0 °C (right-half-filled circles with and without pip) (by Miyaki[3,30]), and in MEK at 35.0 °C (left-

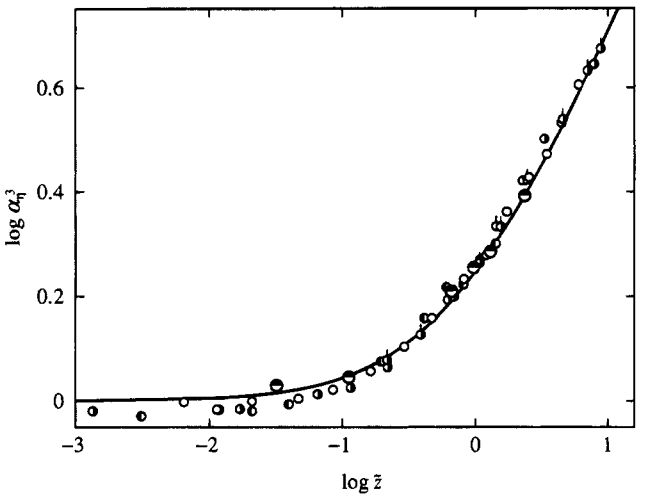

Figure 9. Double-logarithmic plots of α_η^3 against $\tilde{z}$ for a-PS: (◓) in 4-*tert*-butyltoluene at 50.0 °C (present data); (○) in toluene at 15.0 °C (previous data);[2] (◑) in benzene at 25.0 °C (previous data);[3] (●, pip up) in benzene at 25.0 °C (Miyaki);[3,30] (◐) in MEK at 25.0 °C (previous data).[3] The solid curve represents the values calculated from eq 13 with $\tilde{z}$ in place of z.

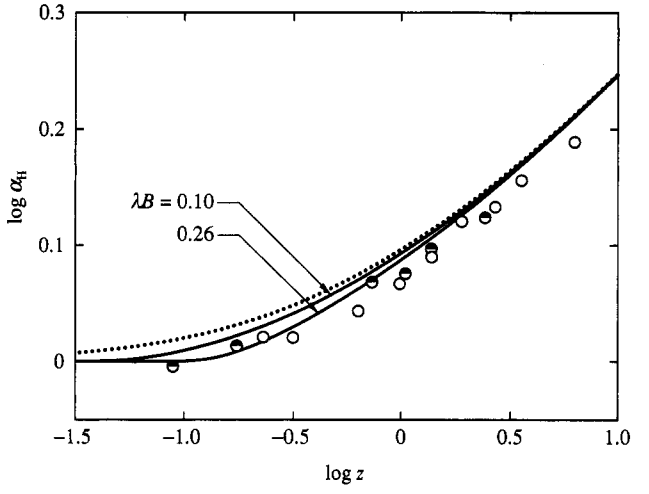

Figure 10. Double-logarithmic plots of α_H against z for a-PS in toluene at 15.0 °C and in 4-*tert*-butyltoluene at 50.0 °C. The symbols have the same meaning as those in Figure 5. The solid curves represent the values calculated from eq 10 with $\tilde{z}$ in place of z, and the dotted curve represents the corresponding f_H-modified two-parameter-theory values (see text).

half-filled circles). The solid curve represents the theoretical values calculated from eq 13 with $\tilde{z}$ in place of z. It is seen that the present data agree with the previous ones, forming a single composite curve. This result reconfirms that α_η is a function only of $\tilde{z}$, or, in other words, the quasi-two-parameter scheme is valid for α_η for a-PS irrespective of the difference in solvent condition (excluded-volume strength).

We are now in a position to examine the behavior of α_H as functions of z and $\tilde{z}$ in comparison with the theoretical prediction. In Figure 10, the values of α_H are plotted double-logarithmically against z with the present data for a-PS in toluene at 15.0 °C (unfilled circles) and in 4-*tert*-butyltoluene at 50.0 °C (top-half-filled circles). The solid curves represent the values calculated from eq 10 with eqs 8 (for $\alpha_H^{(Z)}$), 9, 11, and 12 with $\tilde{z}$ in place of z, and the dotted curve represents the new (f_H-modified) two-parameter theory values calculated from eq 10 similarly (but with $\tilde{z} = z$). It is seen that the solid curves deviate downward progressively

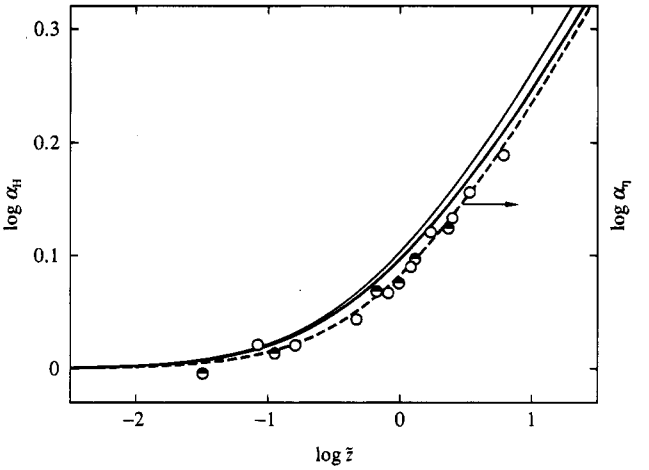

Figure 11. Double-logarithmic plots of α_H against $\tilde{z}$ for a-PS in toluene at 15.0 °C and in 4-*tert*-butyltoluene at 50.0 °C. The symbols have the same meaning as those in Figure 5. The heavy and light solid curves represent the values calculated from eqs 10 and 8 with $\tilde{z}$ in place of z, respectively (see text). The dashed curve represents the values of α_η calculated from eq 13 with $\tilde{z}$ in place of z.

from the dotted curve with decreasing z (or decreasing L) because of the effect of chain stiffness as in the case of α_S and α_η. The effect becomes more significant as λB is increased, or, in other words, as the solvent quality becomes better. The observed values of α_H are seen to become unity at finite z in agreement with the theoretical prediction shown by the solid curves, indicating that the effect of chain stiffness is very significant for α_H as well as for α_S and α_η for small z (or M_w). The data points deviate remarkably downward from the dotted curve over the whole range of z (or M_w) studied. However, this deviation should not be ascribed entirely to the effect of chain stiffness, since the new quasi-two-parameter theory still somewhat overestimates α_H even for large (or intermediate) z, as recognized from the differences between the solid curves and the data points. Thus it is concluded that the new theory may explain the observed results only semiquantitatively.

Figure 11 shows double-logarithmic plots of α_H against $\tilde{z}$ with the same data as those in Figure 10. The light solid curve represents the values of α_H calculated from eq 8, and the heavy solid curve represents those calculated from eq 10 with eqs 8 (for $\alpha_H^{(Z)}$), 9, 11, and 12, both with $\tilde{z}$ in place of z. On the other hand, the dashed curve represents the values of α_η calculated from eq 13 with $\tilde{z}$ in place of z. It is seen that all the data points form a single composite curve over the whole range of M_w studied irrespective of the solvent condition. The implication is that at least for a-PS, α_H becomes a function only of $\tilde{z}$, or, in other words, the quasi-two-parameter scheme is valid also for α_H as well as for α_S and α_η.

As anticipated from the results in Figure 6, the light solid curve deviates progressively upward from the data points with increasing $\tilde{z}$. The deviation is decreased by taking account of the effect of fluctuating HI on α_H, as shown by the heavy solid curve. It is seen that the heavy solid curve is closer to the data points for larger $\tilde{z}$, the deviation being still somewhat large for $0.1 \lesssim \tilde{z} \lesssim 1$. This result suggests that the Barrett equation itself for α_H, i.e., eq 8, used in eq 10 may not be good enough to explain the observed behavior of α_H, although the theory probably overestimates the factor f_H, as already discussed.[13]

It is surprising to see that the data points closely follow the dashed curve, which represents the relation between α_η and $\tilde{z}$, in the range of M_w studied. However, this requires a comment. The factor f_H given by eq 11 with $d/a = 1.0$ becomes 0.88 in the limit of $\tilde{z}$ (or α_S) $\rightarrow \infty$, and then α_H given by eq 10 with eq 8 becomes

$$\lim_{\tilde{z}\rightarrow\infty} \alpha_H = 1.00\tilde{z}^{0.2} \quad (20)$$

The coefficient 1.00 in eq 20 is smaller than that in the corresponding asymptotic form for α_η, i.e.,

$$\lim_{\tilde{z}\rightarrow\infty} \alpha_\eta = 1.07\tilde{z}^{0.2} \quad (21)$$

Thus the heavy solid curve intersects the dashed curve at a certain large value of $\tilde{z}$ and then becomes lower than the latter for larger $\tilde{z}$. This predicts that the value of α_H for very large $\tilde{z}$ might be smaller than that given by the dashed curve if it were actually measured.

Conclusion

In this work, we have investigated α_H as a function of $\tilde{z}$ (and also of α_S) for a-PS with the fraction of racemic diads $f_r = 0.59$ in toluene at 15.0 °C and in 4-*tert*-butyltoluene at 50.0 °C. The values of α_H have been calculated correctly by taking $R_{H,\Theta}$ in cyclohexane at Θ as a reference standard on the basis of the previous[1,18] and present findings that $\langle S^2\rangle_\Theta$ and $R_{H,\Theta}$ in this Θ state coincide with $\langle S^2\rangle_0$ and $R_{H,0}$ in the above solvents, respectively. The present results give the values of α_H appreciably smaller than the values calculated from the Barrett equation,[17] in accordance with the literature results[14-16] for various polymer–solvent systems. It is found that the new Yamakawa–Yoshizaki theory[13] which takes account of the possible effect of fluctuating HI on α_H may explain semiquantitatively the observed results, it still somewhat overestimating α_H.

The present results show that the effect of chain stiffness on α_H is significant as in the case of α_S and α_η.[1-5] It is also shown that α_H as a function of $\tilde{z}$ is independent of solvent, giving a single composite curve over the whole range of M_w studied. This implies that the quasi-two-parameter scheme is valid also for α_H as well as for α_S and α_η. It is very interesting to find that the single composite curve above may be accidentally represented by the Barrett equation[12] for α_η with $\tilde{z}$ in place of z in the range of M_w studied. All of the present findings above should be confirmed for other polymer–solvent systems. This is now in progress.

References and Notes

(1) Abe, F.; Einaga, Y.; Yoshizaki, T.; Yamakawa, H. *Macromolecules* **1993**, *26*, 1884.
(2) Abe, F.; Einaga, Y.; Yamakawa, H. *Macromolecules* **1993**, *26*, 1891.
(3) Horita, K.; Abe, F.; Einaga, Y.; Yamakawa, H. *Macromolecules* **1993**, *26*, 5067.
(4) Abe, F.; Horita, K.; Einaga, Y.; Yamakawa, H. *Macromolecules* **1994**, *27*, 725.
(5) Kamijo, M.; Abe, F.; Einaga, Y.; Yamakawa, H. *Macromolecules* **1995**, *28*, 1095.
(6) Yamakawa, H.; Stockmayer, W. H. *J. Chem. Phys.* **1972**, *57*, 2843.
(7) Yamakawa, H.; Shimada, J. *J. Chem. Phys.* **1985**, *83*, 2607.
(8) Shimada, J.; Yamakawa, H. *J. Chem. Phys.* **1986**, *85*, 591.
(9) Yamakawa, H. *Annu. Rev. Phys. Chem.* **1984**, *35*, 23.
(10) Yamakawa, H. In *Molecular Conformation and Dynamics of Macromolecules in Condensed Systems*; Nagasawa, M., Ed.; Elsevier: Amsterdam, 1988; p 21.
(11) Domb, C.; Barrett, A. J. *Polymer* **1976**, *17*, 179.
(12) Barrett, A. J. *Macromolecules* **1984**, *17*, 1566.
(13) Yamakawa, H.; Yoshizaki, T. *Macromolecules*, preceding paper in this issue.
(14) Varma, B. K.; Fujita, Y.; Takahashi, M.; Nose, T. *J. Polym. Sci., Polym. Phys. Ed.* **1984**, *22*, 1781.
(15) Tsunashima, Y.; Hirata, M.; Nemoto, N.; Kurata, M. *Macromolecules* **1988**, *21*, 1107.
(16) Fetters, L. J.; Hadjichristidis, N.; Lindner, J. S.; Mays, J. W.; Wilson, W. W. *Macromolecules* **1991**, *24*, 3127.
(17) Barrett, A. J. *Macromolecules* **1984**, *17*, 1561.
(18) Yamakawa, H.; Abe, F.; Einaga, Y. *Macromolecules* **1993**, *26*, 1898.
(19) Yamada, T.; Yoshizaki, T.; Yamakawa, H. *Macromolecules* **1992**, *25*, 377.
(20) Konishi, T.; Yoshizaki, T.; Shimada, J.; Yamakawa, H. *Macromolecules* **1989**, *22*, 1921.
(21) Konishi, T.; Yoshizaki, T.; Saito, T.; Einaga, Y.; Yamakawa, H. *Macromolecules* **1990**, *23*, 290.
(22) Einaga, Y.; Koyama, H.; Konishi, T.; Yamakawa, H. *Macromolecules* **1989**, *22*, 3419.
(23) Konishi, T.; Yoshizaki, T.; Yamakawa, H. *Macromolecules* **1991**, *24*, 5614.
(24) Yamakawa, H.; Abe, F.; Einaga, Y. *Macromolecules* **1994**, *27*, 5704.
(25) Yamada, T.; Koyama, H.; Yoshizaki, T.; Einaga, Y.; Yamakawa, H. *Macromolecules* **1993**, *26*, 2566.
(26) Dehara, K.; Yoshizaki, T.; Yamakawa, H. *Macromolecules* **1993**, *26*, 5137.
(27) Sawatari, N.; Konishi, T.; Yoshizaki, T.; Yamakawa, H. *Macromolecules* **1995**, *28*, 1089.
(28) Rossini, F. D.; Pitzer, K. S.; Arnett, R. L.; Braun, R. H.; Pimentel, G. C. *Selected Values of Physical and Thermodynamic Properties of Hydrocarbons and Related Compounds*; Carnegie Press: Pittsburgh, 1953.
(29) Huber, K.; Bantle, S.; Lutz, P.; Burchard, W. *Macromolecules* **1985**, *18*, 1461.
(30) Miyaki, Y. Ph.D. Thesis, Osaka University, 1981.

MA946527B